© 2021 Journal of Pharmacy & Pharmacognosy Research, 9 (5), 730-745, 2021
ISSN 0719-4250
http://jppres.com/jppres

Original Article

Natural products repurposing of the H5N1-based lead compounds for the most fit inhibitors against 3C-like protease of SARS-CoV-2

[Reutilización de productos naturales de compuestos principales basados en H5N1 para los inhibidores más adecuados contra la proteasa similar a 3C del SARS-CoV-2]

Arli Aditya Parikesit*, Rizky Nurdiansyah

Department of Bioinformatics, School of Life Sciences, Indonesia International Institute for Life Sciences, Jl. Pulomas Barat Kav. 88 Jakarta 13210 Indonesia.
*E-mail: arli.parikesit@i3l.ac.id

Abstract

Context: COVID-19 pandemic has caused more than 2.7 million mortality worldwide. Although the COVID-19 vaccine has been developed, the amount is still limited, and very few countries have reached 'herd immunity' level. In this regard, imported and community infections is still happening in the world. In order to complement the vaccine rollout, the drug is still necessary. Up to now, all the COVID-19 drugs in the market are still in emergency use, and their clinical application is still under tight surveillance. Thus, a breakthrough in drug development is necessary. Based on an extensive protein crystallography experiment, it is known that the 3C-like protease of SARS-CoV-2 plays an important role in the pathogenicity of the virus. Several inhibitors have been developed for this protein, including remdesivir that served as the standard in this experiment. However, recent findings in the wet lab also showed possible significant bioactivities for the repurposed influenza, and human rhinovirus leads for SARS-CoV-2. Previous research has developed flavonoid-based leads as H5N1 virus inhibitors.

Aims: To develop lead compounds to inhibit 3C-like protease of SARS-CoV-2 from the existing H5N1 leads.

Methods: The ligands and protein were prepared with energy minimization and the "add protonation" procedure. Then, the QSAR analysis was conducted to determine whether the ligands fit as leads for the 3C-like protease SARS-CoV-2 inhibitor. Molecular docking simulation was deployed for the selected ligand toward the 3C-like protease enzyme. Moreover, the molecular dynamics simulation was devised to examine the protein flexibility of the protease ligands.

Results: It was found that only 9 out of the 19 repurposed H5N1-leads elicited significant QSAR-based properties for general antivirus, influenza antivirus, and antihuman rhinovirus bioactivities. In this regard, the leads were screened further with molecular docking, *in silico* ADME-TOX prediction, and molecular dynamics methods. Based on the further screen, the ligands of M00009235 and M00006834 were selected as lead compounds for 3C-like protease SARS-CoV-2 inhibitors.

Conclusions: The ligands of M00009235 and M00006834 were selected as the best leads for inhibiting 3C-like protease of SARS-CoV-2 based on the virtual screening methods.

Keywords: 3C-like protease; COVID-19; molecular docking; molecular dynamics; SARS-CoV-2.

Resumen

Contexto: La pandemia de COVID-19 ha causado más de 2,7 millones de muertes en todo el mundo. Hasta ahora, todos los medicamentos COVID-19 en el mercado todavía se encuentran en uso de emergencia y su aplicación clínica aún está bajo estricta vigilancia. Por tanto, es necesario un gran avance en el desarrollo de fármacos. Basado en un extenso experimento de cristalografía de proteínas, se sabe que la proteasa de tipo 3C del SARS-CoV-2 juega un papel importante en la patogenicidad del virus. Se han desarrollado varios inhibidores para esta proteína, incluido el remdesivir que sirvió como estándar en este experimento. Sin embargo, hallazgos recientes en el laboratorio también mostraron posibles bioactividades significativas para la influenza reutilizada y los rinovirus humanos para el SARS-CoV-2. Una investigación anterior ha desarrollado líderes basados en flavonoides como inhibidores del virus H5N1.

Objetivos: Desarrollar compuestos líderes para inhibir la proteasa similar a 3C del SARS-CoV-2 de los cables H5N1 existentes.

Métodos: Los ligandos y la proteína se prepararon con el procedimiento de minimización de energía y "agregar protonación". Luego, se llevó a cabo el análisis QSAR para determinar si los ligandos encajaban como conductores para el inhibidor de la proteasa de tipo 3C SARS-CoV-2. Se implementó la simulación de acoplamiento molecular para el ligando seleccionado hacia la enzima proteasa similar a 3C. Además, la simulación de dinámica molecular se diseñó para examinar la flexibilidad proteica de los ligandos de proteasa.

Resultados: Se encontró que solo 9 de los 19 líderes H5N1 reutilizados obtuvieron propiedades significativas basadas en QSAR para las bioactividades antivirus generales, antivirus contra la influenza y contra rinovirus humanos. En este sentido, los líderes se analizaron más con métodos de acoplamiento molecular, predicción *in silico* ADME-TOX y dinámica molecular. Basándose en el cribado adicional, se seleccionaron los ligandos de M00009235 y M00006834 como compuestos principales para los inhibidores de proteasa de tipo 3C SARS-CoV-2.

Conclusiones: Los ligandos de M00009235 y M00006834 se seleccionaron como los mejores conductores para inhibir la proteasa de tipo 3C del SARS-CoV-2 basándose en los métodos de cribado virtual.

Palabras Clave: proteasa de tipo 3C; COVID-19; acoplamiento molecular; dinámica molecular; SARS-CoV-2.

ARTICLE INFO
Received: April 13, 2021.
Received in revised form: May 25, 2021.
Accepted: May 30, 2021.
Available Online: June 4, 2021.

INTRODUCTION

Since WHO declared the COVID-19 as a pandemic, there are more than 123 million confirmed cases and more than 2.7 million deaths (per 24th March, 2021) (WHO, 2021). COVID-19 is an upper respiratory infection disease with specific symptoms such as shortness of breath, taste loss, and fever (Chen et al., 2020). Hence, based on molecular diagnostics, it is already known that SARS-CoV-2 is the virus that causes the COVID-19 disease (WHO, 2020a). SARS-CoV-2 species taxonomy is part of the *Coronaviridae* family, *Coronavirinae* subfamily, and *Betacoronavirus* genus (International Committee on Taxonomy of Viruses, 2021). SARS-CoV-2 is in the identical genus with other epidemic viruses such as SARS-CoV and MERS-CoV that previously cause an epidemic in several regions (Tang et al., 2020). SARS-CoV-2 is a single positive strand (+ss)RNA virus with 11 protein-coding genes, along with 12 expressed proteins (Naqvi et al., 2020). Extensive genome and proteome annotation efforts for SARS-CoV-2 are ongoing and already provide some insight on the possible druggable protein targets (Parikesit 2020). The SARS-CoV-2 has two main target proteins, namely the RdRp and 3C-like protease (Mirza and Froeyen, 2020). The reason is due to the completeness of the structural information in the RCSB database and their important roles in propagating viral maturation along with its replication (Gul et al., 2020; Pormohammad et al., 2020). These aforementioned structural validations serve as a starting point for the current effort for COVID-19 drug development.

As the COVID-19 pandemic is evolving at a dynamics pace, fast and effective drug development strategies are needed. Drug repurposing is considered extensively because it is cheaper, requires less funding, labor, and time to develop (Parikesit and Nurdiansyah, 2020a; Senger et al., 2020; Singh et al., 2020). The repurposed drugs are mainly curated from previous epidemic occurrences such as Ebola, Hepatitis, Influenza, and SARS/MERS. In this regard, remdesivir, chloroquine, hydroxychloroquine, avigan, and dexamethasone are currently under emergency license to use in many countries as repurposed drugs (Bartoli et al., 2021; Dabbous et al., 2021; Lem et al., 2021). However, the clinical trials show mixed and inconclusive results, and this recent improvement has made the WHO reconsider their initial recommendation on those regiments (WHO, 2020b). Moreover, regardless of WHO's decision, remdesivir could be deployed as *in silico* standard, but not the others as there is no available solid reference (Nguyen et al., 2020). Besides drug repurposing, herbal medicine from natural product compounds is heavily invested as well. China is one of the first countries that devises natural products-based leads as COVID-19 drug candidates in the framework of herbal medicine (Luo et al., 2020; Pang et al., 2020). Indonesia and other countries also have published some initiatives, albeit the expansion to the clinical step remains challenging due to regulatory concerns and mainly not in the framework of the herbal leads repurposing (Arba et al., 2020; 2021; Berretta et al., 2020; Harisna et al., 2021; Khan and Al-Balushi, 2020; Wicaksono and Teixeira da Silva, 2020). One of the most extensively studied natural products class is the flavonoid, due to their pre-existing general antiviral properties in many compounds, as well as their deployability in molecular simulation for COVID-19 drug design (Koentjoro et al., 2020; Sukardiman et al., 2020).

Hence, the development of inhibitors of 3C-like protease of SARS-CoV-2 is considered mainstream due to the previous works on SARS-CoV and MERS-CoV drug development (Zhou et al., 2015; Kumar et al., 2016). Interestingly, it was found that broad-spectrum nucleoside inhibitor has shown efficacy against both influenza and SARS-CoV-2 (Sheahan et al., 2020). Although broad-spectrum antivirals are currently under repurposing efforts, the protease inhibitor is becoming the focal point as it plays an important role in the maturation of the SARS-CoV-2 virus (Senger et al., 2020). There is evidence that neuraminidase inhibitors could inhibit the 3C-like protease of SARS-CoV and MERS (Kumar et al., 2016). Naproxen, an influenza drug, has been shown to elicit activity to 3C-like

protein with *in silico* approach (Chiou et al., 2021). Moreover, an extensive clinical trial is underway for the repurposed influenza drugs for COVID-19 (Lem et al., 2021). This striking repurposing opportunity arises due to both influenza and SARS-CoV-2 utilized TMPRSS2 protein for spike protein cleavage (Breining et al., 2021). In this regard, the possibility to repurpose influenza drugs could be catered as previous research already elicited anti-influenza H5N1 flavonoid-based leads with *in silico* approach (Parikesit et al., 2016). The research objective of this study is to develop solid lead compounds from the previous H5N1 flavonoid-based leads as the inhibitor of the 3C-like protease of SARS-CoV-2.

MATERIAL AND METHODS

Protein and ligand preparation

Download the protease 3C-like protein (PDBID: 6Y2E) from RCSB website (https://www.rcsb.org/search). The protein was deployed in accordance with the methodology of previous research that docked with flavonoid class compounds (Adisurja and Parkesit, 2021). Then, the selected lead compounds from the herbalDB 1.0 library in the mol2 format (http://herbaldb.farmasi.ui.ac.id/) were deployed from the previous research with H5N1 protein (Yanuar et al., 2011; Parikesit et al., 2016; Watty et al., 2017; Syahdi et al., 2019). After the files were retrieved, they will be minimized and protonized with Avogadro version 1.2.0. Moreover, further optimization will be done by adding a hydrogen option, along with the auto-optimization tools. The deployed parameters are force field UFF, steps per update 4, and the steepest descent algorithm.

The mol2 file should be converted to SMILE annotation for further processing. Then, use open babel online to convert mol2 to smile: (http://www.cheminfo.org/Chemistry/Cheminformatics/FormatConverter/index.html) (O'Boyle et al., 2011). Moreover, IUPAC name generator for the SMILE annotations should be deployed. The Chemspider database was utilized to search for the SMILE annotation of the compounds (https://www.chemspider.com/) (Ayers, 2012). For the IUPAC name annotations that absent in the Chemspider, MarvinSketch version 21.3 will be deployed to generate the IUPAC preferred names. The structure to name option will be selected, and 'generate preferred IUPAC name' along with 'single fragment mode' options should be selected as well (Csizmadia, 1999; Hanif et al., 2020).

QSAR analysis and molecular docking

The QSAR analysis was conducted by running Way2drug/PASS server to screen for the ligands' bioactivity (http://www.pharmaexpert.ru/ passonline/), and then a tabulation for the related antiviral properties will be generated. The expected bioactivities are general antiviral, general anti-influenza, viral entry inhibitor, and general anti-rhinovirus properties, and they will be annotated further (Lagunin et al., 2000; Permatasari et al., 2020). The docking validation method was deployed with remdesivir as the positive control, and the decoys were retrieved from the DUDE database (Mysinger et al., 2012; Harisna et al., 2021). Further step would be running the Patchdock server of the ligand versus the 3C-like protein for devising the molecular docking simulation (Schneidman-Duhovny et al., 2005). The deployed parameters were clustering of RMSD 4 Å and the default complex type. Then, remdesivir would be utilized as *in silico* standard (Nguyen et al., 2020; Parikesit and Nurdiansyah, 2020a). The 3C-like protein grid box depiction of the binding and sites was deployed accordingly based on the previous research (Adisurja and Parkesit, 2021). Moreover, the ADME-Tox analysis was deployed to observe the pharmacological and toxicity properties. The utilized applications were Toxtree 3.1.0 (http://toxtree.sourceforge.net/) and SWISS-ADME (http://www.swissadme.ch/) (Daina et al., 2017; Benigni et al., 2008). The PLIP server will be deployed to observe the chemical interaction (https://plip-tool.biotec.tu-dresden.de/plip-web/plip/index) (Salentin et al., 2015).

Molecular dynamics

The online molecular dynamics simulation for the best leads was done by CABSFLEX2 (http://biocomp.chem.uw.edu.pl/CABSflex2/ind

ex). It was designed to determine the root-mean-square fluctuation (RMSF) indicator of protein flexibility. It measures the amplitude of atom dynamics during the molecular simulation (Bornot et al., 2011). The parameters should be noted accordingly, namely, the main one that dictates the RMSF of 1-3 Å to indicate stable peptides (Kumar et al., 2019; Uddin et al., 2019). The parameters of distance restrain generator, additional distance restrain, and advanced simulation options will be set as default values (Kuriata et al., 2018).

RESULTS

The protein data of 3C-like protease was directly annotated from previous research and ready to use for the molecular simulation directly (Adisurja and Parkesit, 2021). Moreover, the HerbalDB-based compound annotations were retrieved based upon written agreement with the developer, and those compounds were already assessed in the previous research on H5N1 inhibitors (Yanuar et al., 2011; Parikesit et al., 2016). The complete depiction of the annotated flavonoid compounds could be observed in Table 1. It encompasses various structural diversity, IUPAC names, as well as their ID annotations both in Chemspider or drawn within the framework of the Marvin Sketch application.

The +ssRNA virus infecting respiratory tracts is the hallmark of both human rhinovirus and coronavirus (Greenberg, 2016). Moreover, the similarity of both viruses is striking, as they are utilizing the 3C-like protease for viral maturation (Boozari and Hosseinzadeh, 2021). In this regard, 3C-like protease is becoming a mainstream target for COVID-19 drug development. Although influenza virus is a negative (-)ssRNA virus, the structural and functional homology of both spike and hemagglutinin proteins of influenza and coronavirus are considered relatively significant (Shen et al., 2017). To this end, it could be inferred that COVID-19 inhibitors could be repurposed or redeveloped from existing influenza and rhinovirus leads. This underlying information was mainly annotated in our QSAR analysis result in Fig. 1.

QSAR analysis with PASS server is necessary to validate the suitability of the lead compounds as 3C-like protease inhibitors. In regard to Fig. 1, the threshold of Pa = 0.3-0.7 is considered moderate activity, while above 0.7 is considered highly significant bioactivity (Lagunin et al., 2000; Filimonov et al., 2014). Based on the existence of significant anti-rhinovirus activity, as well as sufficient anti-influenza and general antiviral activities, it is decided to use M00006246, M00009338, M00006834, M00009106, M00014329, M00009235, M00009213, and M00009105 as the lead compounds to do the docking. Anti-rhinoviral leads tend to act as a protease inhibitor, although it is slightly different from SARS-CoV-2 protease. Hence, the docking validation protocol was deployed with 51 decoys. 36 out of 51 were eliciting significantly lower docking scores than remdesivir. The significant functional similarity between human rhinovirus and SARS-CoV-2 protease is the basis of the molecular docking simulation with the designated leads, as depicted in Table 2.

Table 2 depicts the docking score and ACE of the chosen lead compounds. The docking score refers to the geometric shape complementarity score, and the ACE is the abbreviation of the atomic contact energy (Schneidman-Duhovny et al., 2005). The docking score is inversely proportional with the free energy Gibbs (ΔG), while the ACE is proportional to it. In this regard, the leads that inhibited the 3C-like protein with the most favorable parameters are M00009235 and M00006834. Both of them have a better docking score and ACE than the standard and other leads. Although the validated docking simulation already showed promising proposed leads, observing the toxicological properties is still necessary, as shown in Table 3.

In Table 3, almost all annotated compounds exposed moderate toxicity, albeit their crammer rules compliance showed high toxic (class III) compounds, yet all other parameters did not depict significant toxicity. However, the two compounds have notable exceptions. The M00006246 and M00009338 are deemed too toxic as they showed a clear sign of carcinogenicity and positive result in the *in silico* Ames test. Therefore, both of

them are excluded from the further processing of this pipeline. Then, the pipeline progressed further with the *in silico* testing of the general pharmacological properties, as depicted in Table 4.

As depicted in Table 4, all leads consistently show 3 violations of the Lipinski rules. This doesn't mean that the leads are not druggable, as there are many marketed drugs that violated the Lipinski rules significantly (Proudfoot, 2005; Walters, 2012). However, the synthetic accessibility of the compounds is relatively challenging, on the scale of 1 (easiest to synthesize) to 10 (difficult to synthesize). Both of our best compounds have a value of more than 6.70 that will require extensive medicinal chemistry studies for devising the best synthetic route. Hence, after observing the macro-level toxicology and pharmacological indicators, a micro indicator should be catered, namely the chemical interactions that supported the macro indicators. Fig. 2 illustrates the chemical interactions between the 3C-like protease and the ligand leads.

Table 1. The annotated compounds from the HerbalDB database that was computed for the H5N1 virus inhibitor.

No.	Chemical structure	HerbaDB ID	IUPAC name (ChemSpider or Marvin Sketch generated)	ChemSpider ID or Marvin sketch generated
1.	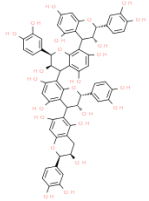	M00009105	(2R,2'R,2''R,2'''R,3R,3'R,3''R,3'''R)-2,2',2'',2'''-Tetrakis(3,4-dihydroxyphenyl)-3,3',3'',3''',4,4',4'',4'''-octahydro-2H,2'H,2''H,2'''H-4,8':4',8'':4'',6'''-quaterchromene-3,3',3'',3''',5,5',5'',5'' ',7,7',7'',7'''-dodecol	17337318
2.	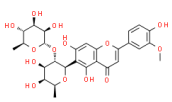	M00014066	(6R)-2,6-Anhydro-1-deoxy-5-O-(6-deoxy-α-L-mannopyranosyl)-6-[5,7-dihydroxy-2-(4-hydroxy-3-methoxyphenyl)-4-oxo-4H-chromen-6-yl]-D-galactitol	8778908
3.	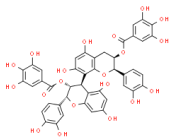	M00009213	(2R,2'R,3R,3'R,4R)-2,2'-Bis(3,4-dihydroxyphenyl)-5,5',7,7'-tetrahydroxy-3,3',4,4'-tetrahydro-2H,2'H-4,8'-bichromene-3,3'-diyl bis(3,4,5-trihydroxybenzoate)	110532
4.	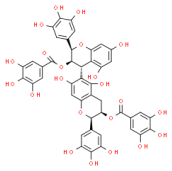	M00009235	(2R,2'R,3R,3'R,4S)-5,5',7,7'-Tetrahydroxy-2,2'-bis(3,4,5-trihydroxyphenyl)-3,3',4,4'-tetrahydro-2H,2'H-4,6'-bichromene-3,3'-diyl bis(3,4,5-trihydroxybenzoate)	410670
5.	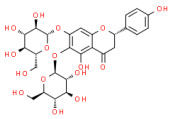	M00014329	(2S)-6-(β-D-Glucopyranosyloxy)-5-hydroxy-2-(4-hydroxyphenyl)-4-oxo-3,4-dihydro-2H-chromen-7-yl β-D-glucopyranoside	58802112
6.	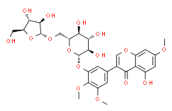	M000019135	5-(5-Hydroxy-7-methoxy-4-oxo-4H-chromen-3-yl)-2,3-dimethoxyphenyl 6-O-α-L-arabinofuranosyl-β-D-glucopyranoside	9290024

Table 1. The annotated compounds from the HerbalDB database that was computed for the H5N1 virus inhibitor (continued...)

No.	Chemical structure	HerbaDB ID	IUPAC name (ChemSpider or Marvin Sketch generated)	ChemSpider ID or Marvin sketch generated
7.	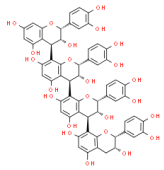	M00009106	Cinnamtannin A2	10272879
8.	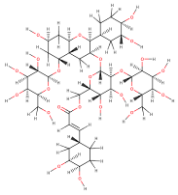	M00006843	[(2S,3S,4S,5S,6S)-6-{[(2S,3S,4aS,5R,7S,8aR)-2-[(1S,3R,4R)-3,4-Dihydroxycyclohexyl]-7-hydroxy-5-{[(2S,3S,4R,5S,6S)-3,4,5-trihydroxy-6-(hydroxymethyl)oxan-2-yl]oxy}-octahydro-2H-1-benzopyran-3-yl]oxy}-3,4-dihydroxy-5-{[(2R,3S,4S,5R,6S)-3,4,5-trihydroxy-6-(hydroxymethyl)oxan-2-yl]oxy}oxan-2-yl]methyl (2E)-3-[(1R,3S,4R)-3,4-dihydroxycyclohexyl]prop-2-enoate	Marvin sketch
9.	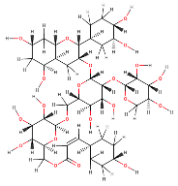	M00006832	[(2S,3R,4S,5S,6S)-6-{[(2S,3R,4R,5R,6S)-6-{[(2R,3R,4aS,5S,7S,8aS)-2-[(1S,3S,4S)-3,4-Dihydroxycyclohexyl]-5,7-dihydroxy-octahydro-2H-1-benzopyran-3-yl]oxy}-3,4-dihydroxy-5-{[(2R,3R,4R,5S)-3,4,5-trihydroxyoxan-2-yl]oxy}oxan-2-yl]methoxy}-3,4,5-trihydroxyoxan-2-yl]methyl (2Z)-3-[(1r,4r)-4-hydroxycyclohexyl]prop-2-enoate	Marvin sketch
10.	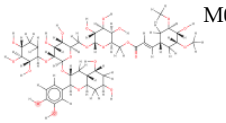	M00006834	4-[(2S,3R,4aR,5R,7R,8aR)-3-{[(2R,3R,4R,5S,6R)-4,5-Dihydroxy-6-({[(2S,3R,4S,5R,6R)-3,4,5-trihydroxy-6-({[(2E)-3-[(1S,3R,4S,5R)-4-hydroxy-3,5-dimethoxycyclohexyl]prop-2-enoyl]oxy}methyl)oxan-2-yl]oxy}methyl)-3-{[(1R,2R,3S,4R)-2,3,4-trihydroxycyclohexyl]oxy}oxan-2-yl]oxy}-5,7-dihydroxy-octahydro-2H-1-benzopyran-2-yl]benzene-1,2-bis(olate)	Marvin sketch
11.	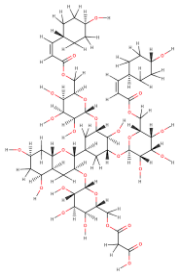	M00014803	3-{[(2R,3S,4R,5S,6R)-6-{[(2R,3S,4aS,5S,7R,8aS)-5,7-Dihydroxy-2-[(1R,3R,4S,5S)-4-hydroxy-3,5-bis({[(2S,3S,4S,5R,6R)-3,4,5-trihydroxy-6-({[(2Z)-3-[(1r,4r)-4-hydroxycyclohexyl]prop-2-enoyl]oxy}methyl)oxan-2-yl]oxy})cyclohexyl]-octahydro-2H-1-benzopyran-3-yl]oxy}-3,4,5-trihydroxyoxan-2-yl]methoxy}-3-oxopropanoic acid	Marvin sketch
12.	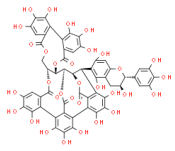	M00009338	(1R,2S,20R,42R,46R)-7,8,9,12,13,14,25,26,27,30,31,32,35,36,37-Pentadecahydroxy-46-[(2R,3S)-3,5,7-trihydroxy-2-(3,4,5-trihydroxyphenyl)-3,4-dihydro-2H-chromen-6-yl]-3,18,21,41,43-pentaoxanonacyclo[27.13.3.138,42.02,20.05,10.011,16.023,28.033,45.034,39]hexatetraconta-5,7,9,11,13,15,23,25,27,29(45),30,32,34,36,38-pentadecaene-4,17,22,40,44-pentone	23327282

Table 1. The annotated compounds from the HerbalDB database that was computed for the H5N1 virus inhibitor (continued...)

No.	Chemical structure	HerbaDB ID	IUPAC name (ChemSpider or Marvin Sketch generated)	ChemSpider ID or Marvin sketch generated
13.	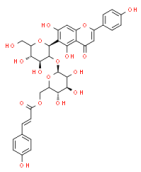	M00014080	(1S)-1,5-Anhydro-1-[5,7-dihydroxy-2-(4-hydroxyphenyl)-4-oxo-4H-chromen-6-yl]-2-O-{6-O-[(2E)-3-(4-hydroxyphenyl)-2-propenoyl]-β-D-threo-hexopyranosyl}-D-threo-hexitol	24843325
14.	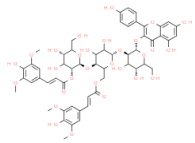	M00005901	5,7-Dihydroxy-2-(4-hydroxyphenyl)-4-oxo-4H-chromen-3-yl 2-O-[(2E)-3-(4-hydroxy-3,5-dimethoxyphenyl)-2-propenoyl]-β-D-erythro-hexopyranosyl-(1->4)-6-O-[(2E)-3-(4-hydroxy-3,5-dimethoxyphenyl)-2-prope noyl]-β-D-glycero-hexopyranosyl-(1->2)-α-L-threo-hexopyranoside	24844443
15.	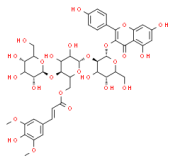	M00005900	5,7-Dihydroxy-2-(4-hydroxyphenyl)-4-oxo-4H-chromen-3-yl β-D-erythro-hexopyranosyl-(1->4)-6-O-[(2E)-3-(4-hydroxy-3,5-dimethoxyphenyl)-2-propenoyl]-β-D-glycero-hexopyranosyl-(1->2)-α-L-threo-h exopyranoside	24844442
16.	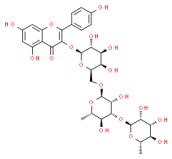	M00013746	Kaempferol-3-galactoside-6''-rhamnoside-3'''-rhamnoside	22912808
17.	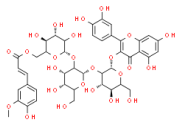	M00013884	2-(3,4-Dihydroxyphenyl)-5,7-dihydroxy-4-oxo-4H-chromen-3-yl 6-O-[(2E)-3-(4-hydroxy-3-methoxyphenyl)-2-propenoyl]-β-D-threo-hexopyranosyl-(1->2)-α-L-erythro-hexopyranosyl-(1->2)-β-D-threo-hex opyranoside	24844985
18.	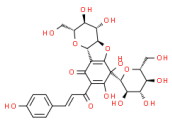	M00006246	(1R)-1,5-Anhydro-1-{(2R,3S,4S,4aR,9bS)-3,4,6,7-tetrahydroxy-2-(hydroxymethyl)-8-[(2E)-3-(4-hydroxyphenyl)-2-propenoyl]-9-oxo-3,4,4a,6,9,9b-hexahydro-2H-pyrano[3,2-b][1]benzofuran-6-yl}-D-glucitol	57257193
19	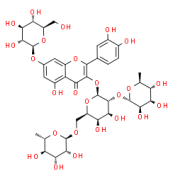	M00005487	2-(3,4-Dihydroxyphenyl)-7-(β-D-glucopyranosyloxy)-5-hydroxy-4-oxo-4H-chromen-3-yl 6-deoxy-α-L-mannopyranosyl-(1->2)-[6-deoxy-α-L-mannopyranosyl-(1->6)]-β-D-galactopyranoside	58918065

The fifth column depicted whether the structure of the lead compounds was annotated in the ChemSpider database or was generated with Marvin sketch chemical structure builder application.

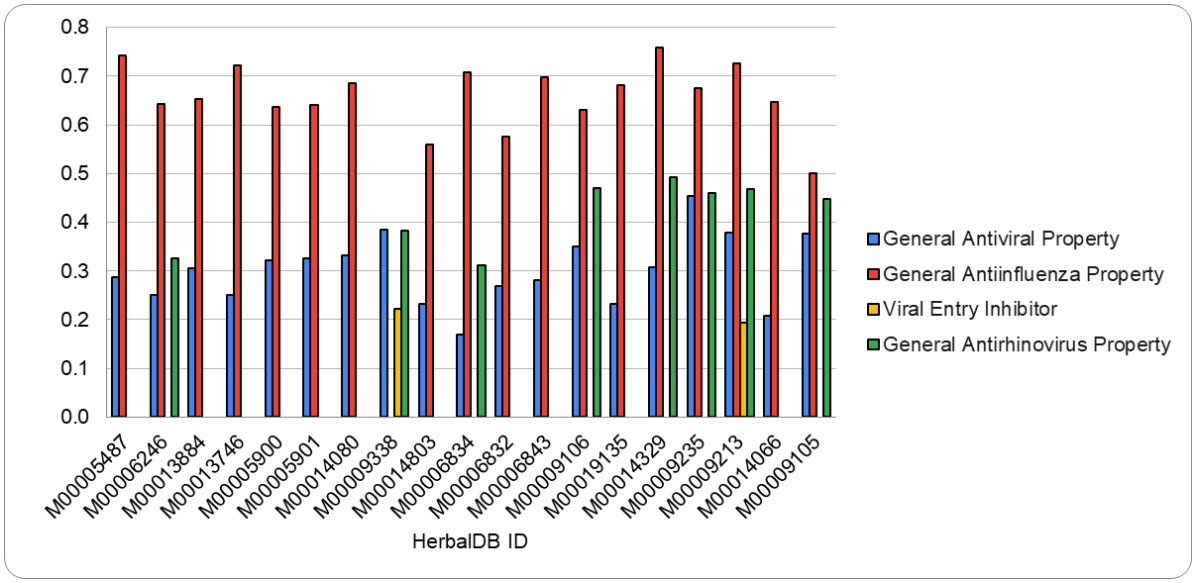

Figure 1. The PASS server output of the selected compounds of H5N1 inhibitors in Table 1.

Y-axis represents the Pa (probability) value, while X-axis represents the herbalDB ID. Different color bars reflect different bioactivities annotation.

Table 2. The PATCHDOCK output of the selected ligands.

No.	HerbalDB ID	Docking score	ACE value
1.	M00006246	5532	-317.92
2.	M00009338	6666	-194.14
3.	M00006834*	7194	-285.30
4.	M00009106	6862	-370.98
5.	M00014329	5618	-282.75
6.	M00009235*	6630	-409.61
7.	M00009213	6734	-381.67
8.	M00009105	7158	-292.57
9.	Remdesivir (standard drug)	6114	-99.09

The score and ACE values are both depicted in the table. *Leads with the most favorable docking score and ACE values. ACE is atomic contact energy that calculated from solvation Delta Gs.

Table 3. The Toxtree output of the selected compounds from Table 2.

No.	Compounds HebarlDB ID	Crammer rules	Carcinogenicity (genotoxic and non-genotoxic) and mutagenicity	*In vitro* mutagenicity (AMES test)	Skin corrosion	Eye irritation
1.	M00009105	High (class III)	Negative for genotoxic carcinogenicity, negative for nongenotoxic carcinogenicity	No alerts for *S. typhimurium* mutagenicity	Not corrosive to the skin	Not eye irritation R36
2.	M00009213	High (class III)	Negative for genotoxic carcinogenicity, negative for nongenotoxic carcinogenicity	No alerts for *S. typhimurium* mutagenicity	Not corrosive to the skin	Not eye irritation R36
3.	M00009235*	High (class III)	Negative for genotoxic carcinogenicity, negative for nongenotoxic carcinogenicity	No alerts for *S. typhimurium* mutagenicity	Not corrosive to the skin	Not eye irritation R36
4.	M00014329	High (class III)	Negative for genotoxic carcinogenicity, negative for nongenotoxic carcinogenicity	No alerts for *S. typhimurium* mutagenicity	Not corrosive to the skin	Not lesions R34, R35, R36, R41
5.	M00009106	High (class III)	Negative for genotoxic carcinogenicity, negative for nongenotoxic carcinogenicity	No alerts for *S. typhimurium* mutagenicity	Not corrosive to the skin	Not eye irritation R36
6.	M00006834*	High (class III)	Negative for genotoxic carcinogenicity, negative for nongenotoxic carcinogenicity	No alerts for *S. typhimurium* mutagenicity	Not corrosive to the skin	Not eye irritation R36
7.	M00009338	High (class III)	Structural alert for genotoxic and nongenotoxic carcinogenicity	Structural alert for *S. typhimurium* mutagenicity	Not corrosive to the skin	Not eye irritation R36
8.	M00006246	High (class III)	Structural alert for genotoxic carcinogenicity	Structural alert for *S. typhimurium* mutagenicity	Not corrosive to the skin	Not eye irritation R36

*Leads with the most favorable docking score and ACE values.

Fig. 2 shows that all lead compounds are hampered by steric effects during their ongoing interaction with the 3C-like protease active sites. After overseeing all the interaction visualizations, only M00009235 (Fig. 2D) leads interaction that shows less constraint from the steric effects due to the more opening in the cavity. M00009235 happens to be one of the best leads from the docking simulation. Although the PLIP run show only the best 3D conformations possible for the protein-ligand complexes, it is clear that only one complex that could relieve the restraint of the steric effects. In order to observe the details of the chemical interaction, Table 5 depicts the total hydrogen bonds in the complex.

Table 5 shows that the interaction complex of M00009106 with 3C-like protease has the most bonds count, while the least is the M00009213. Although M00009235 is not having the most hydrogen bonds count, but reference from Fig. 2D shows that the lead has much less restraint from steric effects. Interestingly, although the M00009106 has the most hydrogen bond count, the M00006834 has a more favorable docking score

and ACE value. Based upon this virtual screening consideration, M00009235 and M00006834 are still considered the top-picked leads. Thus, Fig. 3 depicts the complex visualization between the 3C-like protease with the ligands.

Table 4. SWISSADME output for the selected compounds.

No.	Compound HerbalDB ID	Lipinski rule of 5 (Drug-likeness)	Synthetic accessibility
1.	M00006834*	No; 3 violations: MW>500, NorO>10, NHorOH>5	9.16
2.	M00009106	No; 3 violations: MW>500, NorO>10, NHorOH>5	8.58
3.	M00014329	No; 3 violations: MW>500, NorO>10, NHorOH>5	6.25
4.	M00009235*	No; 3 violations: MW>500, NorO>10, NHorOH>5	6.70
5.	M00009213	No; 3 violations: MW>500, NorO>10, NHorOH>5	6.65
6.	M00009105	No; 3 violations: MW>500, NorO>10, NHorOH>5	8.58

*Leads with the most favorable docking score and ACE values.

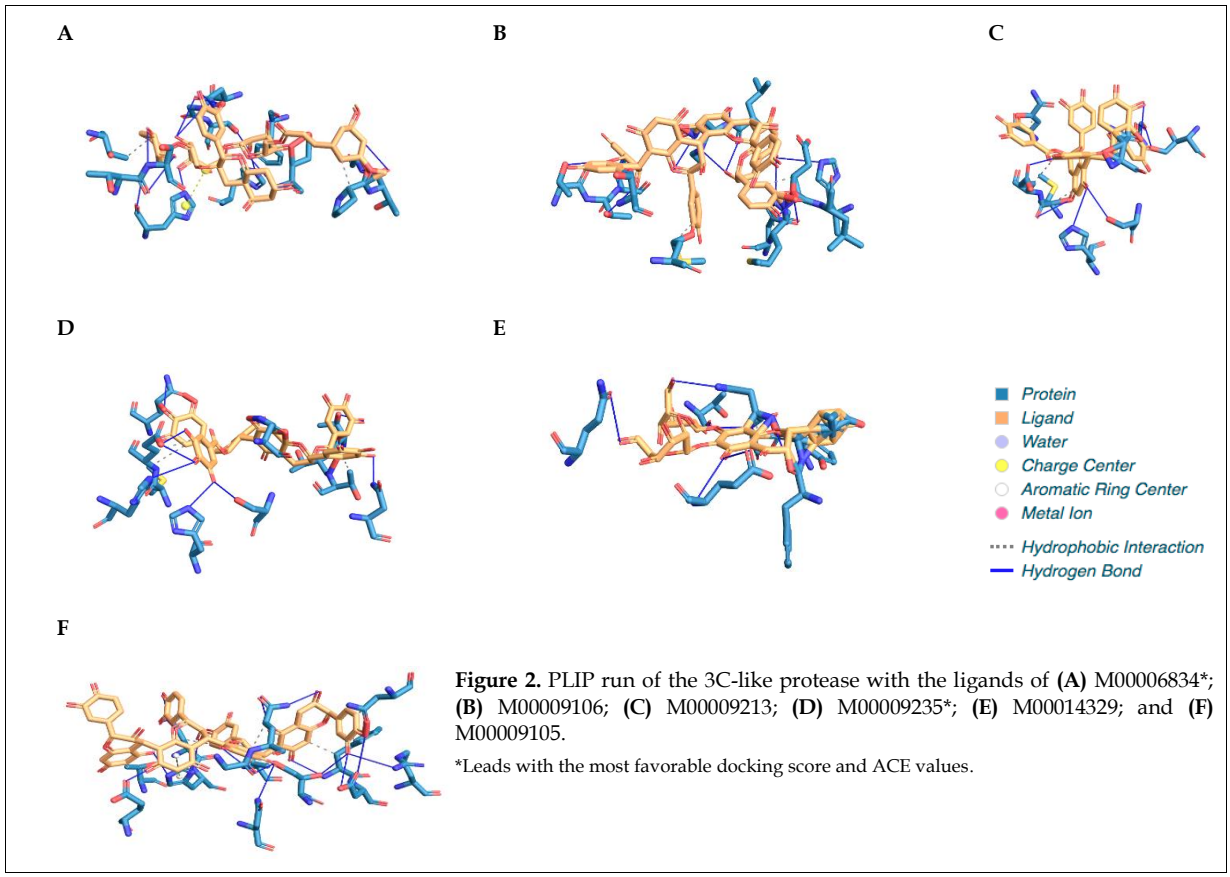

Figure 2. PLIP run of the 3C-like protease with the ligands of **(A)** M00006834*; **(B)** M00009106; **(C)** M00009213; **(D)** M00009235*; **(E)** M00014329; and **(F)** M00009105.

*Leads with the most favorable docking score and ACE values.

Table 5. The hydrogen bond between the amino acid (AA) residues of the 3C-like protease and the ligands.

No.	HerbalDB ID	Hydrogen bonds in the AA residues (total bonds count)
1.	M00006834*	HIS41, THR45, SER46, PHE140, ASN142, GLY143, SER144, HIS163, GLU166, THR169, GLY170 (11)
2.	M00009106	THR24, THR25, THR26, SER46, LEU141, ASN142, GLY143, HIS163, MET165, GLU166, LEU167, HIS172 (12)
3.	M00009213	CYS44, ASN142, SER144, HIS163, MET165, GLU166 (6)
4.	M00009235*	THR24, THR26, ASN119, ASN142, SER144, HIS163, GLU166, HIS172, GLN189 (9)
5.	M00014329	THR26, PHE140, ASN142, GLY143, GLU166, GLN189 (6)
6.	M00009105	GLY109, GLN110, ASN203, GLU240, ASP245, HIS246, THR292, PHE294, ASP295, ARG298 (10)

*Leads with the most favorable docking score and ACE values.

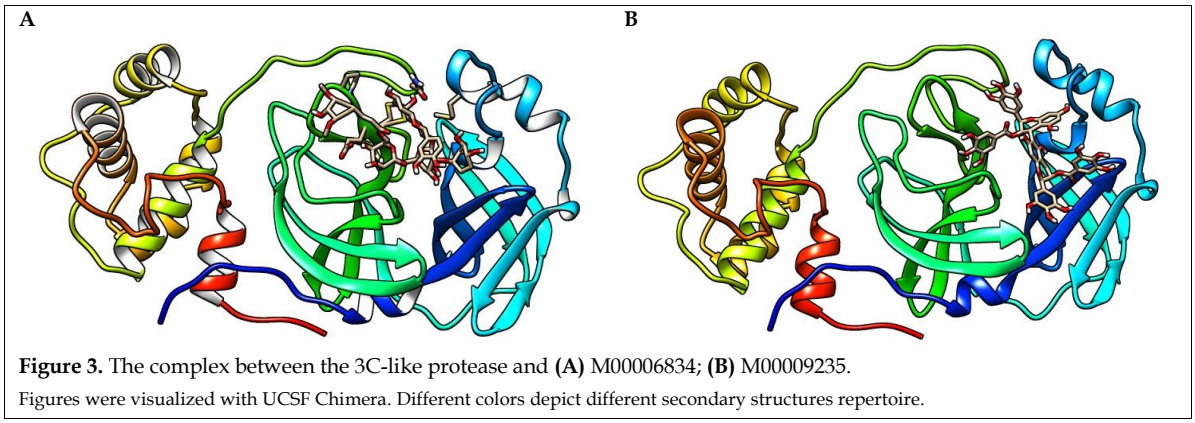

Figure 3. The complex between the 3C-like protease and **(A)** M00006834; **(B)** M00009235.
Figures were visualized with UCSF Chimera. Different colors depict different secondary structures repertoire.

Fig. 3 shows mainly the alpha-helix and beta-sheet secondary structure depiction evenly. However, it is clear that due to the different conformation of the ligand bindings, the protein conformations are different as well. The ligands are visualized in the center, albeit both are providing different stereochemical conformations. These different conformations will, in turn providing different protein flexibility dynamics, as seen in Fig. 4. Both 3C-like protease complexes with M00009235 and M00006834 have the lowest free energy and the highest score possible.

As seen in Fig. 4, the protein fluctuations are still falling under the RMSF threshold of 1-3 Å. To this end, they are still considered in a stable conformation. However, there is a slightly different RMSF fluctuation between the inhibition of 3C-like protease with M00009235 and M00006834. The protease-M00009235 complex has significant fluctuation in amino acid residue number 46-61, while the protease-M00009235 has that on residue number 106. The difference in the RMSF fluctuation shows that the difference of ligand conformations will eventually affect the protein flexibility as well.

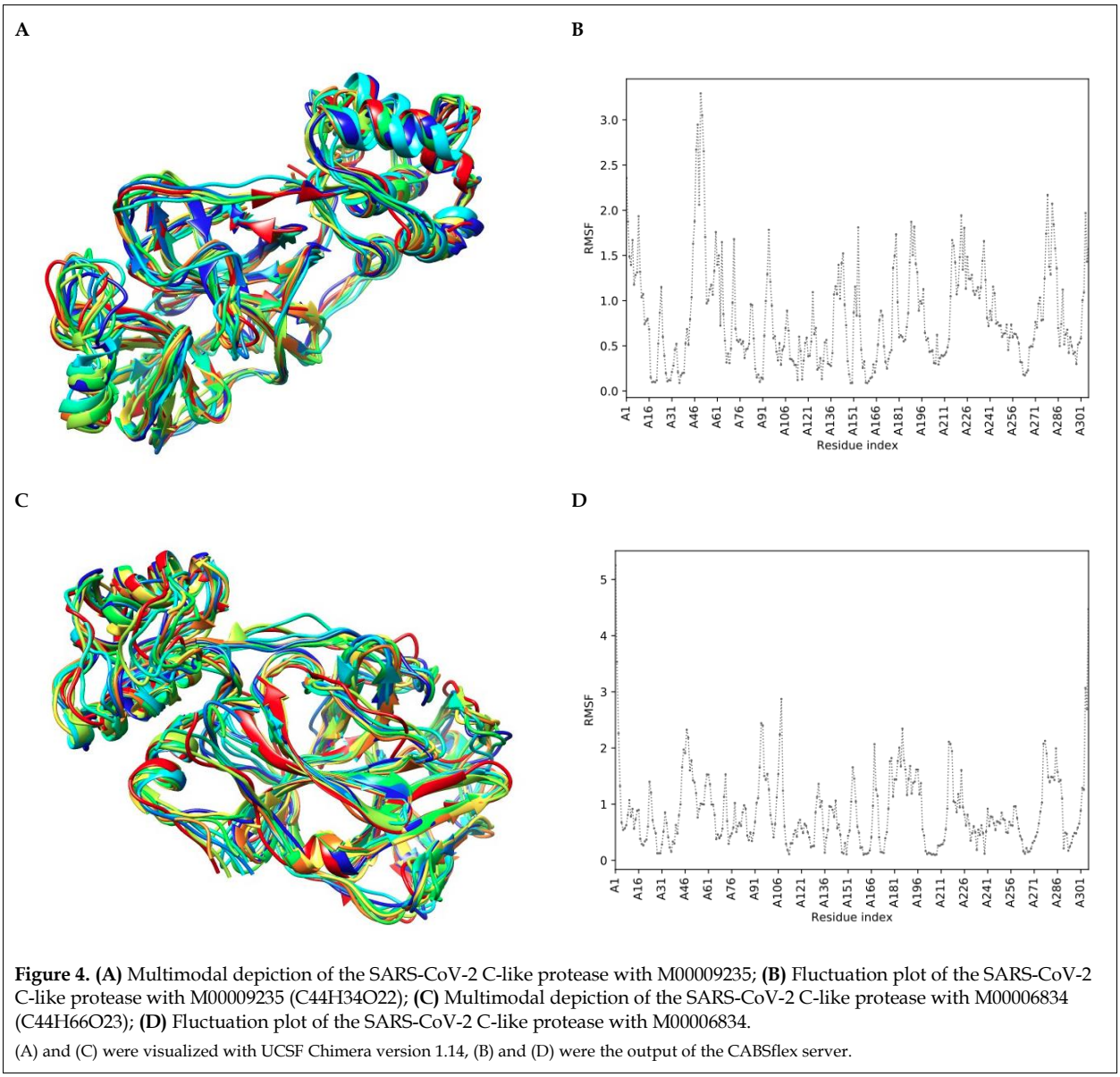

Figure 4. (A) Multimodal depiction of the SARS-CoV-2 C-like protease with M00009235; **(B)** Fluctuation plot of the SARS-CoV-2 C-like protease with M00009235 (C44H34O22); **(C)** Multimodal depiction of the SARS-CoV-2 C-like protease with M00006834 (C44H66O23); **(D)** Fluctuation plot of the SARS-CoV-2 C-like protease with M00006834.

(A) and (C) were visualized with UCSF Chimera version 1.14, (B) and (D) were the output of the CABSflex server.

DISCUSSION

The virtual screening methods are eliciting thorough computational iterations to obtain the best possible leads. Many of the standard tools could be accessed online, and even the computationally extensive molecular dynamics could be conducted online. Offline computational efforts are mainly conducted for basic data biocuration efforts. The extensive screenings have produced annotations that both M00009235 and M00006834 leads are deemed as the best leads. In this regard, it is clear that this *in silico* pipeline has emphasized the reusability of the H5N1 leads as SARS-CoV-2 inhibitors.

Investigating the possible protein-protein or protein-RNA interaction within the existing SARS-CoV-2 proteins is definitely becoming an interesting option due to the importance of this study, albeit with limited existing data sets (Ramanto and Parikesit, 2019). Further research should be devised in curating the interaction of 3C-like protease with other proteins and other biomolecules like DNA and non-coding RNA. One of the landmarks of this research is the structural and func-

tional similarity between SARS-CoV-2 and human rhinovirus protease enzyme. The functional assay to prove the dual inhibition of those enzymes has been devised in the wet lab setting (Liu et al., 2021). Then, there is a possibility that human rhinovirus infection could hamper the SARS-CoV-2 replication in the respiratory epithelium due to interferon up-regulation that signifies deterrence toward viral infections (Dee et al., 2021). Some recent findings also showed that human rhinovirus infection could inhibit SARS-CoV-2 inoculation during *in vitro* experiments (Dee et al., 2021). This finding could serve as a biomedical basis to repurpose human rhinovirus inhibitors for SARS-CoV-2. In this regard, further studies for the repurposed rhinovirus inhibitors for SARS-CoV-2 are necessary, especially more thorough studies in the wet lab.

Moreover, it is clear that actually, the flavonoid compounds have elicited significant *in vitro* bioactivity toward SARS (SARS-CoV) and MERS virus (Nguyen et al., 2012; Jo et al., 2020; Russo et al., 2020). Those findings were actually serving as a pharmaceutical chemistry basis to extrapolate the leads for the SARS-CoV-2 virus, as both MERS and SARS-CoV belong to the same genus with SARS-CoV-2.

This study could be devised as a compromise between purely drug repurposing and natural products research for developing COVID-19 drugs, especially in the interest of promoting herbal medicine (Lim et al., 2019). There will be no contradiction as both studies are catered to in this effort (Rastelli et al., 2020). Natural product repurposing could be elicited as the efficient and effective approach to promote local biodiversity (Byun et al., 2019). Thus, a protein-based drug is not the sole strategy for COVID-19 treatment. Developing an RNA-based drug is also an option (Parikesit and Nurdiansyah, 2020b). However, developing herbal leads are important to preserve the local wisdom of one's country. China is one interesting example as they are the earliest party that published herbal-based SARS-CoV-2 inhibitors based on a bioinformatics approach (Ang et al., 2020; Luo et al., 2020; Pang et al., 2020). However, other countries are following closely and have established a natural products-based library as well for COVID-19 lead compounds (Berretta et al., 2020; Khan and Al-Balushi, 2020). To this end, the various lead compound proposals will enable the scientific community to conduct much more thorough research for devising a conclusive COVID-19 drug lead.

CONCLUSIONS

The repurposed H5N1 ligands from the HerbalDB database were curated for the SARS-CoV-2 3C-like protease inhibitors, and significant amounts have elicited promising results. The QSAR method has significantly converged the optimized ligands accordingly in order to focus on developing the most promising leads. Thus, the molecular simulations pipeline has successfully elicited the leads accordingly. In this regard, the selected best ligands are M00009235 and M00006834 due to their proven stability during molecular docking and dynamics methods. Both ligands also elicit satisfactory in silico ADME-TOX properties.

CONFLICT OF INTEREST

The authors declare no conflicts of interest.

ACKNOWLEDGMENTS

The authors would like to thank the Institute of Research and Community Empowerment (LPPM) of Indonesia International Institute for Life Sciences (i3L) for supporting this study. The authors would like to thank also the Deputi Bidang Penguatan Riset dan Pengembangan, Kementerian Riset dan Teknologi dan LLDIKTI3 for providing Hibah Penelitian Dasar 2021 No. B/112/E3/RA.00/2021.

REFERENCES

Adisurja GP, Parkesit AA (2021) Virtual screening of the flavonoids compounds with the SARS-CoV-2 3C-like protease as the lead compounds for the COVID-19. Coronaviruses 02: 1. DOI: 10.2174/2666796702666210222105547

Ang L, Song E, Lee HW, Lee MS (2020) Herbal medicine for the treatment of Voronavirus Disease 2019 (COVID-19): A systematic review and meta-analysis of randomized controlled trials. J Clin Med 9(5): 1583.

Arba M, Nur-Hidayat A, Usman I, Yanuar A, Wahyudi ST, Fleischer G, Brunt DJ, Wu C (2020) Virtual screening of the Indonesian medicinal plant and zinc databases for

potential inhibitors of the RNA-dependent RNA polymerase (RdRp) of 2019 novel coronavirus. Indones J Chem 20(6): 1430.

Arba M, Wahyudi ST, Brunt DJ, Paradis N, Wu C (2021) Mechanistic insight on the remdesivir binding to RNA-dependent RNA polymerase (RdRp) of SARS-COV-2. Comput Biol Med 129: 104156.

Ayers M (2012) ChemSpider: The Free Chemical Database. Ref Rev 26(7): 45–46.

Bartoli A, Gabrielli F, Alicandro T, Nascimbeni F, Andreone P (2021) COVID-19 treatment options: a difficult journey between failed attempts and experimental drugs. Intern Emerg Med 16(2): 281–308.

Benigni R, Bossa C, Jeliazkova N, Netzeva T, Worth A (2008) The Benigni/Bossa rulebase for mutagenicity and carcinogenicity – a module of Toxtree. EUR 23241 EN. Luxembourg: OPOCE. JRC43157.

Berretta AA, Silveira MAD, Cóndor Capcha JM, De Jong D (2020) Propolis and its potential against SARS-CoV-2 infection mechanisms and COVID-19 disease. Biomed Pharmather 131: 110622.

Boozari M, Hosseinzadeh H (2021) Natural products for COVID-19 prevention and treatment regarding to previous coronavirus infections and novel studies. Phyther Res 35(2): 864–876.

Bornot A, Etchebest C, De Brevern AG (2011) Predicting protein flexibility through the prediction of local structures. Proteins 79(3): 839–852.

Breining P, Frølund AL, Højen JF, Gunst JD, Staerke NB, Saedder E, Cases-Thomas M, Little P, Nielsen LP, Søgaard OS, Kjolby M (2021) Camostat mesylate against SARS-CoV-2 and COVID-19—Rationale, dosing and safety. Basic Clin Pharmacol Toxicol 128(2): 204–212.

Byun MR, Lee DH, Jang YP, Lee HS, Choi JW, Lee SK (2019) Repurposing natural products as novel HDAC inhibitors by comparative analysis of gene expression profiles. Phytomedicine 59: 152900.

Chen T, Wu D, Chen H, Yan W, Yang D, Chen G, Ma K, Xu D, Yu H, Wang H, Wang T, Guo W, Chen J, Ding C, Zhang X, Huang J, Han M, Li S, Luo X, Zhao J, Ning Q (2020) Clinical characteristics of 113 deceased patients with coronavirus disease 2019: retrospective study. BMJ 368: m1091.

Chiou WC, Hsu MS, Chen YT, Yang JM, Tsay YG, Huang HC, Huang C (2021) Repurposing existing drugs: identification of SARS-CoV-2 3C-like protease inhibitors. J Enzyme Inhib Med Chem 36(1): 147–153.

Csizmadia P (1999) MarvinSketch and MarvinView: Molecule Applets for the World Wide Web. The 3rd International Electronic Conference on Synthetic Organic Chemistry session Information and Compound Archives Management and Internet Application, [E0002]. Basel, Switzerland: MDPI, p. 1775.

Dabbous HM, Abd-Elsalam S, El-Sayed MH, Sherief AF, Ebeid FFS, El Ghafar MSA, Soliman S, Elbahnasawy M, Badawi R, Tageldin MA (2021) Efficacy of favipiravir in COVID-19 treatment: a multi-center randomized study. Arch Virol 166(3): 949–954.

Daina A, Michielin O, Zoete V (2017) SwissADME: a free web tool to evaluate pharmacokinetics, drug-likeness and medicinal chemistry friendliness of small molecules. Sci Rep 7(1): 42717.

Dee K, Goldfarb DM, Haney J, Amat JAR, Herder V, Stewart M, Szemiel AM, Baguelin M, Murcia PR (2021) Human rhinovirus infection blocks SARS-CoV-2 replication within the respiratory epithelium: implications for COVID-19 epidemiology. J Infect Dis 23: jiab147.

Filimonov DA, Lagunin AA, Gloriozova TA, Rudik A V., Druzhilovskii DS, Pogodin PV, Poroikov VV (2014) Prediction of the biological activity spectra of organic compounds using the pass online web resource. Chem Heterocycl Comp 50(3): 444–457.

Greenberg SB (2016) Update on human rhinovirus and coronavirus infections. Semin Respir Crit Care Med 37(4): 555–571.

Gul S, Ozcan O, Asar S, Okyar A, Barıs I, Kavakli IH (2020) *In silico* identification of widely used and well-tolerated drugs as potential SARS-CoV-2 3C-like protease and viral RNA-dependent RNA polymerase inhibitors for direct use in clinical trials. J Biomol Struct Dyn 2020: 1–20.

Hanif AU, Lukis PA, Fadlan A (2020) Pengaruh minimisasi energi MMFF94 dengan MarvinSketch dan open Babel PyRx pada penambatan molekular turunan oksindola tersubstitusi. Alchemy 8(2): 33–40.

Harisna AH, Nurdiansyah R, Syaifie PH, Nugroho DW, Saputro KE, Firdayani, Prakoso CD, Rochman NT, Maulana NN, Noviyanto A, Mardliyati E (2021) *In silico* investigation of potential inhibitors to main protease and spike protein of SARS-CoV-2 in propolis. Biochem Biophys Rep 26: 100969.

International Committee on Taxonomy of Viruses (2021) ICTV Master Species List 2019 v1. Checklist dataset https://doi.org/10.15468/i4jnfv accessed via GBIF.org on 2021-03-31.

Jo S, Kim S, Shin DH, Kim MS (2020) Inhibition of SARS-CoV 3CL protease by flavonoids. J Enzyme Inhib Med Chem 35(1): 145–151.

Khan SA, Al-Balushi K (2020) Combating COVID-19: The role of drug repurposing and medicinal plants. J Infect Public Health 14(4): 495–503.

Koentjoro MP, Donastin A, Prasetyo EN (2020) Potensi senyawa bioaktif tanaman kelor penghambat interaksi angiotensin-converting enzyme 2 pada sindroma SARS-COV-2. J Bioteknol Biosains Indones 7(2): 259–270.

Kumar N, Sood D, Tomar R, Chandra R (2019) Antimicrobial peptide designing and optimization employing large-scale flexibility analysis of protein-peptide fragments. ACS Omega 4(25): 21370–21380.

Kumar V, Tan KP, Wang YM, Lin SW, Liang PH (2016) Identification, synthesis and evaluation of SARS-CoV and

MERS-CoV 3C-like protease inhibitors. Bioorganic Med Chem 24(13): 3035–3042.

Kuriata A, Gierut AM, Oleniecki T, Ciemny MP, Kolinski A, Kurcinski M, Kmiecik S (2018) CABS-flex 2.0: A web server for fast simulations of flexibility of protein structures. Nucleic Acids Res 46(W1): W338–343.

Lagunin A, Stepanchikova A, Filimonov D, Poroikov V (2000) PASS: prediction of activity spectra for biologically active substances. Bioinformatics 16(8):747–748.

Lem FF, Opook F, Lee DJH, Chee FT, Lawson FP, Chin SN (2021) Molecular mechanism of action of repurposed drugs and traditional Chinese medicine used for the treatment of patients infected with COVID-19: a systematic scoping review. Front Pharmacol 11: 2413.

Lim DW, Kim H, Kim YM, Chin YW, Park WH, Kim JE (2019) Drug repurposing in alternative medicine: herbal digestive Sochehwan exerts multifaceted effects against metabolic syndrome. Sci Rep 9(1): 9055.

Liu C, Boland S, Scholle MD, Bardiot D, Marchand A, Chaltin P, Blatt LM, Beigelman L, Symons JA, Raboisson P, Gurard-Levin ZA, Vandyck K, Deval J (2021) Dual inhibition of SARS-CoV-2 and human rhinovirus with protease inhibitors in clinical development. Antiviral Res. 187: 105020.

Luo X, Ni X, Lin J, Zhang Y, Wu L, Huang D, Liu Y, Guo J, Wen W, Cai Y, Chen Y, Lin L (2020) The add-on effect of Chinese herbal medicine on COVID-19: a systematic review and meta-analysis. Phytomedicine 85: 153282.

Mirza MU, Froeyen M (2020) Structural elucidation of SARS-CoV-2 vital proteins: Computational methods reveal potential drug candidates against main protease, Nsp12 polymerase and Nsp13 helicase. J Pharm Anal 10(4): 320–328.

Mysinger MM, Carchia M, Irwin JJ, Shoichet BK (2012) Directory of useful decoys, enhanced (DUD-E): Better ligands and decoys for better benchmarking. J Med Chem 55(14): 6582–6594.

Naqvi AAT, Fatima K, Mohammad T, Fatima U, Singh IK, Singh A, Atif SM, Hariprasad G, Hasan GM, Hassan MI (2020) Insights into SARS-CoV-2 genome, structure, evolution, pathogenesis and therapies: Structural genomics approach. Biochim Biophys Acta Mol Basis Dis 1866(10): 165878.

Nguyen HL, Thai NQ, Truong DT, Li MS (2020) Remdesivir strongly binds to both RNA-dependent RNA polymerase and main protease of SARS-COV-2: Evidence from molecular simulations. J Phys Chem B 124(50): 11337–11348.

Nguyen TTH, Woo H-JJ, Kang H-KK, Nguyen VD, Kim YM, Kim DW, Ahn SA, Xia Y, Kim D (2012) Flavonoid-mediated inhibition of SARS coronavirus 3C-like protease expressed in *Pichia pastoris*. Biotechnol Lett 34(5): 831–838.

O'Boyle NM, Banck M, James CA, Morley C, Vandermeersch T, Hutchison GR (2011) Open Babel: An open chemical toolbox. J Cheminform 3(1): 33.

Pang W, Liu Z, Li N, Li Y, Yang F, Pang B, Jin X, Zheng W, Zhang J (2020) Chinese medical drugs for coronavirus disease 2019: a systematic review and meta-analysis. Integr Med Res 9(3): 100477.

Parikesit A (2020) Protein domain annotations of the SARS-CoV-2 proteomics as a blue-print for mapping the features for drug and vaccine designs. J Mat Sains 25(2): 26–32.

Parikesit AA, Ardiansah B, Handayani DM, Tambunan USF, Kerami D (2016) Virtual screening of Indonesian flavonoid as neuraminidase inhibitor of influenza a subtype H5N1. IOP Conf Ser Mater Sci Eng 107(1): 012053.

Parikesit AA, Nurdiansyah R (2020a) Drug repurposing option for COVID-19 with structural bioinformatics of chemical interactions approach. Cermin Dunia Kedokt 47(3): 222–226.

Parikesit AA, Nurdiansyah R (2020b) The predicted structure for the anti-sense siRNA of the RNA polymerase enzyme (RdRp) gene of the SARS-CoV-2. Berita Biol 19(1): 97-108.

Permatasari GW Putranto RA, Widiastuti H (2020) Structure-based virtual screening of bioherbicide candidates for weeds in sugarcane plantation using *in silico* approaches. Menara Perkeb 88(2): 100–110.

Pormohammad A, Monych N, Turner R (2020) Zinc and SARS-CoV-2: A molecular modeling study of Zn interactions with RNA-dependent RNA-polymerase and 3C-like proteinase enzymes. Int J Mol Med 47(1): 326–334.

Proudfoot JR (2005) The evolution of synthetic oral drug properties. Bioorganic Med Chem Lett 15(4): 1087–1090.

Ramanto KN, Parikesit AA (2019) The binding prediction model of the iron-responsive element binding protein and iron-responsive elements. Bioinforma Biomed Res J 2(1): 12–20.

Rastelli G, Pellati F, Pinzi L, Gamberini MC (2020) Repositioning natural products in drug discovery. Molecules 25(5): 1154.

Russo M, Moccia S, Spagnuolo C, Tedesco I, Russo GL (2020) Roles of flavonoids against coronavirus infection. Chem Biol Interact 328: 109211.

Salentin S, Schreiber S, Haupt VJ, Adasme MF, Schroeder M (2015) PLIP: Fully automated protein-ligand interaction profiler. Nucleic Acids Res 43(W1): W443–447.

Schneidman-Duhovny D, Inbar Y, Nussinov R, Wolfson HJ (2005) PatchDock and SymmDock: Servers for rigid and symmetric docking. Nucleic Acids Res 33(Suppl. 2): W363–367.

Senger MR, Evangelista TCS, Dantas RF, Santana MVDS, Gonçalves LCS, de Souza Neto LR, Ferreira SB, Silva-Junior FP (2020) COVID-19: molecular targets, drug repurposing and new avenues for drug discovery. Mem Inst Oswaldo Cruz 115: e200254.

Sheahan TP, Sims AC, Zhou S, Graham RL, Pruijssers AJ, Agostini ML, Leist SR, Schäfer A, Dinnon KH 3rd,

Stevens LJ, Chappell JD, Lu X, Hughes TM, George AS, Hill CS, Montgomery SA, Brown AJ, Bluemling GR, Natchus MG, Saindane M, Kolykhalov AA, Painter G, Harcourt J, Tamin A, Thornburg NJ, Swanstrom R, Denison MR, Baric RS (2020) An orally bioavailable broad-spectrum antiviral inhibits SARS-CoV-2 in human airway epithelial cell cultures and multiple coronaviruses in mice. Sci Transl Med 12(541): 5883.

Shen LW, Mao HJ, Wu YL, Tanaka Y, Zhang W (2017) TMPRSS2: A potential target for treatment of influenza virus and coronavirus infections. Biochimie 142: 1–10.

Singh TU, Parida S, Lingaraju MC, Kesavan M, Kumar D, Singh RK (2020) Drug repurposing approach to fight COVID-19. Pharmacol Rep 72(6): 1479–1508.

Sukardiman, Ervina M, Fadhil Pratama M, Poerwono H, Siswodihardjo S (2020) The coronavirus disease 2019 main protease inhibitor from *Andrographis paniculata* (Burm.f) Ness. J Adv Pharm Technol Res 11(4): 157.

Syahdi RR, Iqbal JT, Munim A, Yanuar A (2019) HerbalDB 2.0: Optimization of construction of three-dimensional chemical compound structures to update Indonesian medicinal plant database. Pharmacogn J 11(6): 1189–1194.

Tang D, Comish P, Kang R (2020) The hallmarks of COVID-19 disease. PLoS Pathog 16(5): e1008536.

Uddin MZ, Li X, Joo H, Tsai J, Wrischnik L, Jasti B (2019) Rational design of peptide ligands based on knob-socket protein packing model using CD13 as a prototype receptor. ACS Omega 4(3): 5126–5136.

Walters WP (2012) Going further than Lipinski's rule in drug design. Expert Opin Drug Discov 7(2): 99–107.

Watty M, Syahdi RR, Yanuar A (2017) Database compilation and virtual screening of secondary metabolites derived from marine fungi as epidermal growth factor receptor tyrosine abstract kinase inhibitors. Asian J Pharm Clin Res 10(17): 142.

WHO (2020a) Diagnostic testing for SARS-CoV-2. Geneva.

WHO (2020b) Therapeutics and COVID-19. Geneva.

WHO (2021) WHO Coronavirus Disease (COVID-19) Dashboard.

Wicaksono A, Teixeira da Silva JA (2020) Is COVID-19 impacting plant science, and is plant science impacting COVID-19? Not Sci Biol 12(3): 769–772.

Yanuar A, Mun'im A, Lagho ABA, Syahdi RR, Rahmat M, Suhartanto H (2011) Medicinal plants database and three dimensional structure of the chemical compounds from medicinal plants in Indonesia. Int J Comput Sci 8(5): 180–183.

Zhou Y, Vedantham P, Lu K, Agudelo J, Carrion R Jr, Nunneley JW, Barnard D, Pöhlmann S, McKerrow JH, Renslo AR, Simmons G (2015) Protease inhibitors targeting coronavirus and filovirus entry. Antiviral Res 116: 76–84.

AUTHOR CONTRIBUTION:

Contribution	Parikesit AA	Nurdiansyah R
Concepts or ideas	x	x
Design	x	x
Definition of intellectual content	x	x
Literature search	x	
Experimental studies	x	x
Data acquisition	x	x
Data analysis	x	
Statistical analysis	x	x
Manuscript preparation	x	x
Manuscript editing	x	x
Manuscript review	x	x

Citation Format: Parikesit AA, Nurdiansyah R (2021) Natural products repurposing of the H5N1-based lead compounds for the most fit inhibitors against 3C-like protease of SARS-CoV-2. J Pharm Pharmacogn Res 9(5): 730–745.